DRY-OUT LIMITS AND HEAT TRANSFER PERFORMANCE OF INCLINED HEAT PIPES WITH DIFFERENT HELICAL WIRE WICKS.

Mohamed A. Aziz

Mechanical Power Engineering Department,
Faculty of Engineering - Zagazig University

ABSTRACT

An experimental investigation was conducted to determine the dry-out limitations and the heat transfer performance of four helical wire wicked heat pipes of evaporator, condenser and adiabatic lengths of 25, 25, and 15 cm respectively,. The influences of the wick geometry and inclination angle on the dry-out limitations and overall heat transfer coefficient are considered. The heat pipes were provided with four helical wicks made of 2.5 mm diameter copper wire. The helix pitch investigated were 3,4,5 and 6 mm. Inclination angle was varied from $\psi = 0°$ to $90°$.

The mechanism describing the processes of bubble formation, growth and separation from different geometries of the wicked surface was highlighted. A larger heat transfer rate is achieved with closer helix pitch wicked heat pipe operating with lower vapor temperature and smaller temperature drops. Additional increase in heat transfer coefficient was found with larger inclination angle.

Keywords: Inclined, Helical Wire Wicked, Heat Pipe

NOMENCLATURE

A	area[m^2]
d	diameter [m]
F	flow friction coefficient [Pa/Wm]
(fRe)	drag coefficient,
g	gravitational acceleration[m/s^2]
h_{fg}	latent heat of vaporization[J/kg]
K	permeability[m^2]
k	thermal conductivity [W/mK]
L	length[m]
$\Delta P_{c\ max}$	maximum capillary pressure [Pa]
ΔP_l	pressure drop in liquid phase [Pa]
ΔP_v	pressure drop in vapor phase [Pa]
ΔP_{rh}	radial hydrostatic pressure drop[Pa]
ΔP_{ah}	axial hydrostatic pressure drop[Pa]
Q	heat transfer limit[W]
q	heat flux [W/m^2]
r	radius [m]
s	helix pitch[mm]
T	temperature[K]
U	overall heat transfer coefficient[W/m^2 K]

Subscripts

a	adiabatic
b	boiling
c	capillary - condenser
e	evaporator
e-c	evaporator-condenser
eff	effective
e c	effective-capillary
h	helical
hl	wick hydraulic
L	length, [m]
hv	vapor core hydraulic
HP	heat pipe
i	inner
l	liquid
m	metal
max	maximum
n	normal nucleation
o	outer
t	total
v	vapor, vapor core
w	wick , wire

Greek Symbols

μ	viscosity[kg/ms.]
ρ	density [kg/m^3]
surface tension[N/m]	
δ	liquid film thickness[m]
ψ	inclination angle [deg]
ϕ	wetting angle [rad]
ε	wick porosity [%]

INTRODUCTION

Heat pipes are highly reliable and efficient energy transport devices, which can operate fully passive, with no moving parts or external pumping of working fluid. A heat pipe is a closed heat transfer system, generally in the form of a simple cylindrical pipe sealed at both ends and partially filled with a working fluid. It consists of three basic sections: an evaporator for heat input, adiabatic section and a condenser for heat rejection. The heat pipe operates on the principle of the evaporation of the liquid phase of the working fluid at the heat source (evaporator section) and condensation of the vapor phase of the working fluid at the sink of heat (condenser section).

The latent heat released in the condenser is transferred through the walls of the heat pipe to the exterior surfaces and subsequently to the environment. The condense is then returned back to the evaporator section by the capillary action of the wick structure attached to the pipe wall.

The purpose of a wick is to provide: (i) the necessary flow passages for the return of the condensed liquid, (ii) the surface pores at the liquid vapor interface for the development of the required capillary pumping pressure and (iii) a heat flow path between the inner wall of the container and the liquid vapor interface.

The performance of a heat pipe can be determined by the individual performances of its components including the condenser, the evaporator and the wick.

The heat pipe has been traditionally studied as a system in which case the various design and operating parameters commonly uses screen matrix as a wick structure.

Several studies have been focused on the various operating conditions which include capillary, boiling, sonic, entrainment, and viscous limits. In such studies a screen matrix was used as wick structure [1-4]. A combined experimental and analytical study has been performed by Babin et al. [5] to measure heat transfer capillary limit of a micro heat pipe. Following the same way, a high-temperature sodium/stainless steel heat pipe with multiple heat sources and sinks was used by Faghri et al. [6,7]. A simple circumferemental screen matrix wick of two wraps of 100 mesh per inch was installed to provide a liquid return passage to the evaporator. The tests showed that supersonic vapor velocities occur in the condenser section and no evaporator dryout-capillary limit were found for single or multiple evaporator operation in air or under vacuum. Operational characteristics and performance limitations of four flexible bellows heat pipes having 40 mm in length and 6 mm in diameter were studied by Babin [8]. In this study, the evaporator wick was constructed from 200 mesh per inch copper wire screen. The contribution of El-Genk [9-11] was devoted to study the transient response of heat pipes by a modeling approach. This study was verified experimentally using water as a working fluid and screen matrix as the wick structure. Entrainment phenomena in capillary driven heat pipes were studied by Kim and Peterson [12]. Both analytical and experimental approaches were utilized to clarify the parameters governing the entrainment in operating heat pipes. Mughal and Plumb [13] reported that, the performance of heat pipe may be improved by using an interrupted wick surface as opposed to a solid porous surface, in such manner that interrupted wicked surface may delay the onset of film boiling which, in turn improves, the heat transfer and capillary limit. In this concern, an analytical model for predicting peak dryout steady state heat transfer limits in the heat pipe utilizing sintered-wick structure was presented by Pruzan et al. [14]. The experimental dry-out heat flux values agree to within 10 % with those predicted by the proposed model. Following the same approach, Stephan and Busse [15] presented a model for the radial heat transfer of a grooved heat pipe evaporator wall. The model combines the solution of a two-dimensional heat conduction problem with the calculation of the shape of the liquid-vapor interface and its temperature. A new flat miniature heat pipe configuration utilized for cooling of electronic components was proposed by Khrustalev and Faghri [16]. The tested heat pipe contains an inverted meniscus type evaporator and the axial capillary grooves were covered with a porous plate for the liquid transport. The previous survey leads to the conclusion that the greatest number of reported studies have been concerned with

screen matrix structured heat pipes. The screen matrix wick complicates the boiling process in that it provides additional nucleation sites. In such wicks the liquid is vaporized at the edge of the vapor-filled layer near the heated surface. The generated bubble finds its way out of the wick by flowing along the surface and escapes through the larger pores. If the heat flux is increased, bubble would experience increased difficulty in leaving the surface resulting in a thicker vapor layer and a higher temperature difference. This can be avoided by using an interrupted wicked surface. This surface can be formed by threading the inside wall of the heat pipe using a single point cutting tool to give a thread pitch of up to 4 threads per cm . These threaded arteries are attractive for circumfermental liquid distribution.

An alternative interrupted arrangement is in the form of circular annular wick manufactured form of helical wire.

The objective of this work is to study experimentally the dry-out limits and the heat transfer performance of four helical wire wicks of various geometries. Attention is also focused on the influence of inclination angle on the heat pipe performance.

EXPERIMENTS

Test Facility

A test facility consists of five subsystems (the tested heat pipes a variable heat source, a cooling sink, the measuring instrumentation and a vacuum and charging unit) was constructed in the Mechanical Power Engineering Department of the Faculty of Engineering Zagazig University. The test stand shown in Figure1, enabled tests to be conducted at inclination angles between the horizontal and vertical positions.

In this investigation, four heat pipes of the same dimensions and provided with wicks of different geomerties had been considered. The heat pipe was fabricated from brass tubing with inner and outer diameters of 20 and 26 mm, respectively. The evaporator, adiabatic and condenser lengths are 250, 150, and 250 mm, respectively. The outer surface of the heated section (evaporator) was covered by a silk fabric-electric insulating material, then, a 500 W nickel-chrome ribbon heater was wrapped circumferentially around the entire length of the evaporator to apply uniform heat flux at the evaporator surface. The heater was then covered with an aluminum foil sheet followed by 50 mm thickness of glass-wool thermal insulating material having aluminized outer surface. This design minimizes the heat losses during the experiments to a minimum level and permits taking only the heat generated by the heater into account. The power to the heater was supplied from the building A-C mains and was adjusted by means of an A-C variac transformer. In the condenser, the heat was rejected to the water-coolant-circulating in the cooling jacket. The cooling jacket was made of a PVC tubing with outer and inner diameters of 40 and 36 mm, respectively. The cooling jacket was fed from the building water mains via a flow control valve, by means of which the water flow rate was adjusted.

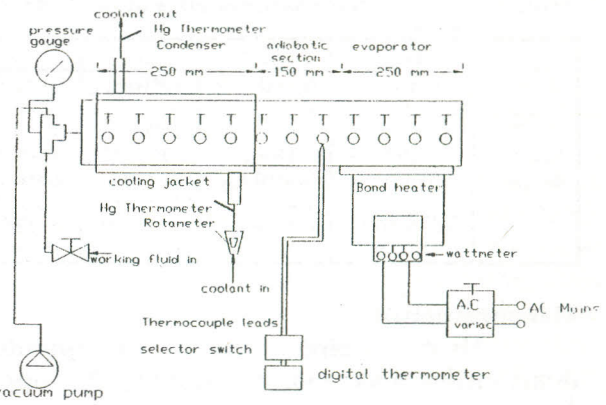

Figure 1 Schematic diagram of the pipe test facility

The entire length of the heat pipe including the cooling jacket was then insulated by glass wool material of 50 mm thickness, and covered by an aluminum foil sheet. Accordingly, the overall energy transfer rate can be calculated either by measuring the rate of energy added by electrical heater or the energy removed by the cooling water. These two measurements were found to agree to within $\pm$ 5 % deviation and provided a check for the insulation condition during the experiments.

Four helical copper wire wicks were manufactured from 2.5 mm diameter wire with identical helix outer diameter of 19 mm but with helix pitch of 3 , 4 , 5 and 6 mm, Figure 2. The corresponding heat pipes are labeled as HP1, HP2, HP3 and HP4, respectively. The geometrical characteristics

of the wick structures are listed in Table 1. Having inserted the helical wick inside the pipe, the terminal ends were inserted into two specially drilled holes and were fixed by soldering.

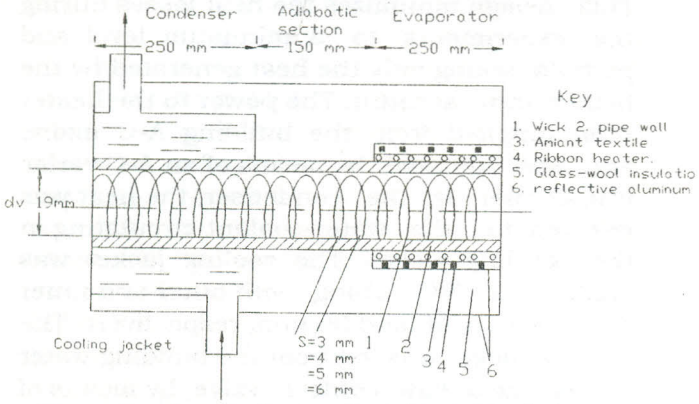

Figure 2 Longitudinal section of tested heat pipe

Table 1 **Geometrical characteristics of the helical wicks**

	HP1	HP2	HP3	HP4
d_h, m	19*10-3	19*10-3	19*10-3	19*10-3
S , mm	3	4	5	6
ε	0.911	0.8	0.732	0.680
K, m²	2.9-10-7	1.15-10-7	8.8-10-8	7.6-10-8
d_w , m	2.5*10-3	2.5*10-3	2.5*10-3	2.5*10-3
$r_{e.c}$, m	5*10-4	1.5*10-3	2.5*103	3.5*10-3
$r_{h.l}$, m	3.698-10-4	6.37-10-4	8.47-10-4	10.136.10-4

Measurements

Heat pipe wall temperature distribution was monitored using 20 copper-constantan thermocouples. The thermocouple junctions were installed at equal intervals of 6 cm in two special grooves cut along the entire length of the heat pipe outer surface. The grooves with thermocouples were covered by a highly resistive powdered copper epoxy mixture. Temperature measurements were also made at the inlet and outlet of the water jacket using mercury in glass thermometers. The thermocouple leads were connected to a change-over switch and the temperature readings was recorded by a type. "Sense Digi" thermometer, accurate to within ± 0.1°C .

In order to determine the rate of energy removed in the cooling jacket, the mass flow rate of the cooling water was measured by a variable area rotameter which was previously calibrated and found to be accurate to within ± 2 % .

The electric power input to the electric heater was measured directly using a digital BRI 5040 type wattmeter, having an uncertainty of 1 % of indicated readings.

These measurements errors resulted in an uncertainty of about ±4% in determining the effective power throughput of the heat pipe.

Experimental Procedure

After the installation of the thermocouples and the heater, the heat pipe parts were carefully fitted and cleaned using the following standard procedure outlined in reference [18] the heat pipe shell and parts were degreased by benzene, followed by alcohol and finally by distilled water and allowed to a jet of dry air. The heat pipe was then evacuated to about 0.01 torr. After that, the heat pipe was charged with 30 cm³ of distilled water which was poured and adjusted using hypodermic syringe.

The heat pipe was set at the selected inclination to the horizontal, and the coolant flow rate was adjusted to a predetermined value. The electric heater was turned on and was set to about 25 W. The system was then allowed to reach the steady state condition. Tests indicated that a time of approximately 60 minutes was necessary for the heat pipe to reach the steady state. During this time, the necessary adjustments in power and coolant flow rates were made. Once the steady state was reached, readings of the temperature, input power and coolant flow rate were recorded.

To obtain data for the successive power values the heat flux was incremented and measurements were repeated, for the heat flux in the range of 1000 to 10000 W/m². This procedure was olso followed for inclination angles ranging between 0 and 90 degrees.

OPERATIONAL CRITERIA

During steady state operation of a heat pipe, the working fluid in the vapor phase flows from the evaporator to the condenser and returns in the form of liquid phase to the evaporator. This is due to the capillary force acting in the wick and creating pressure difference across the liquid-vapor interface.

In general, the operational conditions - or limits - which are needed to be satisfied for a heat pipe under steady state and low temperature situations [5,7 and 8] are usually

governed by the dry-out capillary and boiling limits.

Axial Dry-Out (Capillary Limit)

To satisfy the capillary limit, the capillary pressure difference across the liquid-vapor interface in the heat pipe must be equal to or greater than the total pressure losses throughout the liquid and vapor pathes and the hydrostatic effects. This necessities that :

$$\Delta P_c \geq \Delta P_{rh} + \Delta P_{ah} + \Delta P_l + \Delta P_v \qquad (1)$$

Here, ΔP_c is the capillary pressure difference along the wick length and is derived from Laplace-Young equation. It can be approximated as :

$$\Delta P_c = 2\sigma_l \left(\frac{\cos\phi_e}{r_{ec}} - \frac{\cos\phi_c}{r_c} \right) \qquad (2)$$

Based on Dunn and Ray [18] and Ivanovski et al. [19], the wetting angle between the liquid and wick in the evaporator section $\phi_e = 0$, whereas the corresponding angle in the condenser section ϕ_c is equal to $\pi/2$. At these conditions, ΔP_c will have its maximum value. That is :

$$\Delta P_{c_{max}} = \frac{2\sigma_l}{r_{e.c}} \qquad (3)$$

Here, $r_{e.c}$ is the effective capillary radius of the evaporator wick.

The radial and axial hydrostatic pressure drops are the results of the body forces and can be expressed as :

$$\Delta P_{rh} = \rho_l g\, d_v \cos\psi \qquad (4)$$

$$\Delta P_{ah} = \rho_l g\, L_t \sin\psi \qquad (5)$$

The liquid pressure drop, ΔP_l can be found by evaluating the shear forces at the liquid solid and liquid-vapor interfaces as follows:

$$\Delta P_l = (\mu_l / K.A_w h_{fg} . \rho_l) . L_{eff} . q_c \qquad (6)$$

where, L_{eff} and K are the effective length and permeability respectively, and are expressed as:

$$L_{eff} = L_a + (L_e + L_c)/2 \qquad (7)$$

$$K = \frac{4}{180} \frac{r_{hl}^2\, \varepsilon^3}{(1-\varepsilon)^2} \qquad (8)$$

Here, r_{hl} is the wick hydraulic radius, calculated as given in [15] .

The vapor pressure drop ΔP_v, can be calculated by the expression suggested by both Chi [17] and Dunn and Ray [18] as :

$$\Delta P_v = \left(\frac{(f_v R_{ev})\ \mu_v}{(2\, r_{hv})^2\, A_v . \rho_v\, h_{fg}} \right) L_{eff} . q_c \qquad (9)$$

In Equation 9, r_{hv} is the vapor core hydraulic radius. Simplifying and substituting the relationship for each pressure term and using the conventional method presented by Chi [17], one obtains an expression for the capillary (axial) limit as :

$$(Q)_{cap} = \frac{(\frac{2\sigma}{r_{ec}}) - \rho_l g (d_v \cos\psi - L\sin\psi)}{(F_l + F_v) L_{eff}} \qquad (10)$$

Here, F_l and F_v are the liquid and vapor friction coefficients, respectively, and are defined as :

$$F_l = \mu_l / KA_w \rho_l h_{fg} \qquad (11)$$

$$F_v = (f_v . R_{ev}) \mu_v / 2A_v . r_{hv}^2 \rho_v . h_{fg} \qquad (12)$$

In Equation 10 , the angle of inclination ψ is postulated to be negative when the evaporator is beneath the condenser.

Radial Dry-Out (Boiling) Limit

In the evaporator section, the bubble formation occurs usually on the heated surface. On increasing the radial heat flux bubbles may be formed in the evaporator wick pores. When radial heat flux exceeds a critical value the grown bubbles may coalesce. This in turn, may hinder the liquid return to the heated section and leads to evaporator dry-out. Thus, there is a heat flux limit for the heat pipe evaporator and is termed as the boiling limit. The boiling limit is restricted to the evaporator section and depends on the radial heat flux and differs from the capillary limit which belongs to the axial heat flux limitations.

Using Clauses-Clapeyron equation relating the temperature and the pressure along the saturation line, an expression for the boiling limit had been derived by Chi [17] as:

$$Q_b = \frac{2\pi L_e\, k_{eff}\, T_v}{2h_{fg} . \rho_v . \ln(r_i / r_v)} \left(\frac{2\sigma}{r_n}\right) \qquad (13)$$

where r_n is the nucleation site radius. For conventional heat pipes, r_n can be assumed in the order of $2.54.10^{-5}$ to $2.54*10^{-7}$m. In addition, k_{eff} is the effective thermal conductivity of the liquid-wick combination. k_{eff} can be determined following the procedure outlined by Shoomak [20], as follows :

$$k_{eff} = k_w + [1 - \frac{1}{(1+C)^2}] k_l \qquad (14)$$

Here, C is the specific heat of the working fluid. In addition, k_l and k_w are the thermal conductivities of the working fluid and the wick structure, respectively. The term k_w is calculated taking, into account the wick characteristics, ε as :

$$k_w = (1.85 \cdot \varepsilon \cdot k_m + 8.95\, k_l) / (1 + C)^2 \qquad (15)$$

In this equation, k_m is the thermal conductivity of the wick material.

RESULTS AND DISCUSSION

The results obtained in this investigation include: (1)Analysis of the effects of the wick geometry and operating parameters on the dry-out limits and, (2) analysis of the heat transfer performance in terms of the studied parameters.

The Thermal Conditions

The operating or vapor temperature of a heat pipe is of interest in understanding its heat transport limits and thermal performance. This temperature was determined from measured values of evaporator and condenser temperatures, T_e and T_c , respectively. Based on Huang and Tsuei [5] for the conditions of $L_e = L_c$ the vapor temperature T_v can be taken as, $(T_e + T_c)/2$.

Repeatability tests were also performed for several cases to check the reliability of the experimental setup. In all tests, good repeatability was demonstrated. For example, the heat pipe HP3 test was performed with a total input power of 124 W and the heat pipe reached the steady state with a transport vapor temperature of 52.06°C . On repeating this test with the same input power, the heat pipe reached the steady state with a transport vapor temperature of 51.9 °C .

The experimental data presented in Figure.3 displays the variation of operating (vapor) temperature as a function of the heat flux for the heat pipes: HP1 and HP4 setted the horizontal and vertical positions. It is noticeable that trends of the data are similar. Increasing the heat flux results in a corresponding increase in the operating temperature. An increase in the heat flux causes the liquid meniscus to recede into the channels formed by the helical wire of the wick. This results in a decrease in the radius of curvature of the liquid-vapor meniscus, and a corresponding decrease in the cross-sectional area of the liquid and hence, a slight increase in the evaporator temperature is resulted. The receding of the liquid meniscus continues with increasing power until dryout of the evaporator occurs.

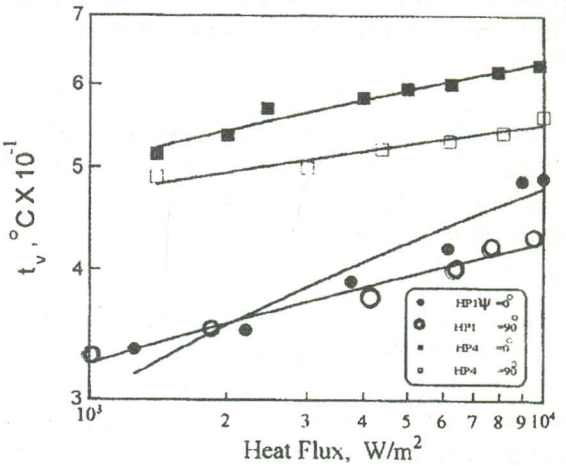

Figure 3 The vapor temperature va. heat flux.

On analyzing Figure 3, one can come to a conclusion that, lower values of T_v are experienced by the HP1 for which a larger liquid flow rate -as it will be shown later- is resulted. It is also seen that the higher vapor temperatures belong to HP4. A horizontal pipe is seen to produce higher vapor temperatures than those obtained with the same pipe when fixed vertically. This gives a crucial idea about the effect of inclination angle ψ on the operating vapor temperature. It reflects the fact that the gravitational effect is very weak in returning the liquid to the evaporator section at ψ = 0. The variation of the evaporator wall-vapor temperature drop (ΔT_{e-v}) , with heat flux is shown in Figure. 4 , while the variation of evaporator - condenser temperature drop (ΔT_{e-c}) , is shown in Figure.5 . Results in both figures indicate tendency regarding the heat flux and inclination angle. Lower temperature drops (ΔT_{e-v}) and (ΔT_{e-c}) were experience by the (HP1) whereas the highest values of these temperature drops are belonging to the (HP4). Thus, one may conclude that an increase in the evaporator temperature would certainly result in significantly higher temperature drops ΔT_{e-v} and ΔT_{e-c} .

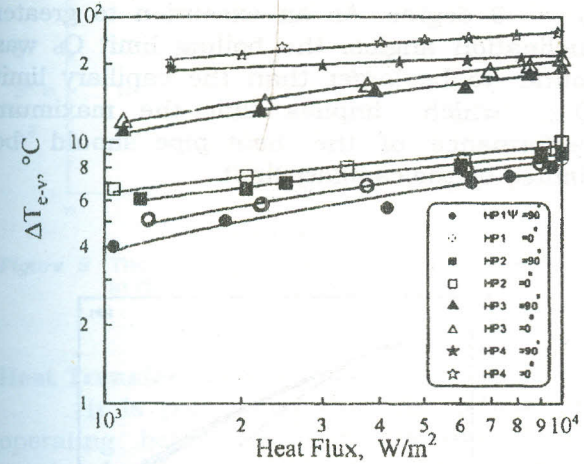

Figure 4 Evaporator-condenser temperature difference va. heat flux

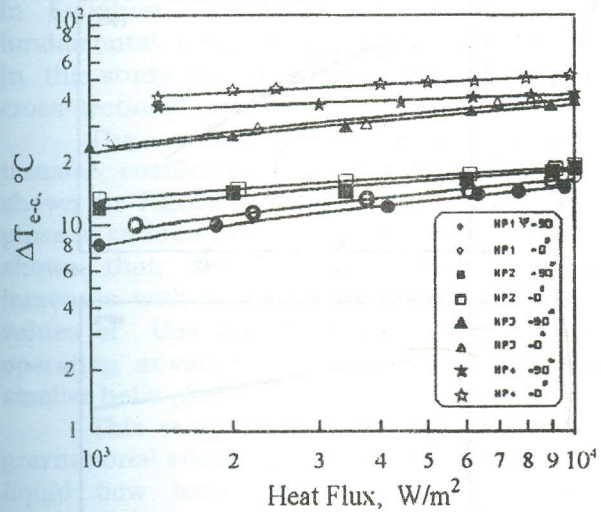

Figure 5 Evaporator-condenser temperature difference vs. heat flux

The Capillary Limit

The capillary limit calculated by Equation 10 is presented in Figure 6 as a function of the operating temperature T_v for the tested heat pipes. The obtained data presented in Figure.6 for ψ=0 show that, at an equal operating temperature, the maximum capillary limit belongs to the HP1. The predicted capillary limit is seen to decrease with increase in the helix pitch as can be seen from the results of the other tested pipes. This can be attributed to the conjugate effects of both the capillary effective radius and the surface tension force. The HP1 has a small capillary radius compared with other test pipes and operates at a relatively small operating temperature, i.e, increased surface tension. This leads to the fact that the contribution of $(\Delta P_c)_{max}$ to the Q_{cap} in Equation 10 becomes more significant. Moreover, the higher permeability of the HP1 leads to a lower flow resistance in the wick and thus, to higher capillary heat transport capacity. Conversely, a large effective capillary radius -

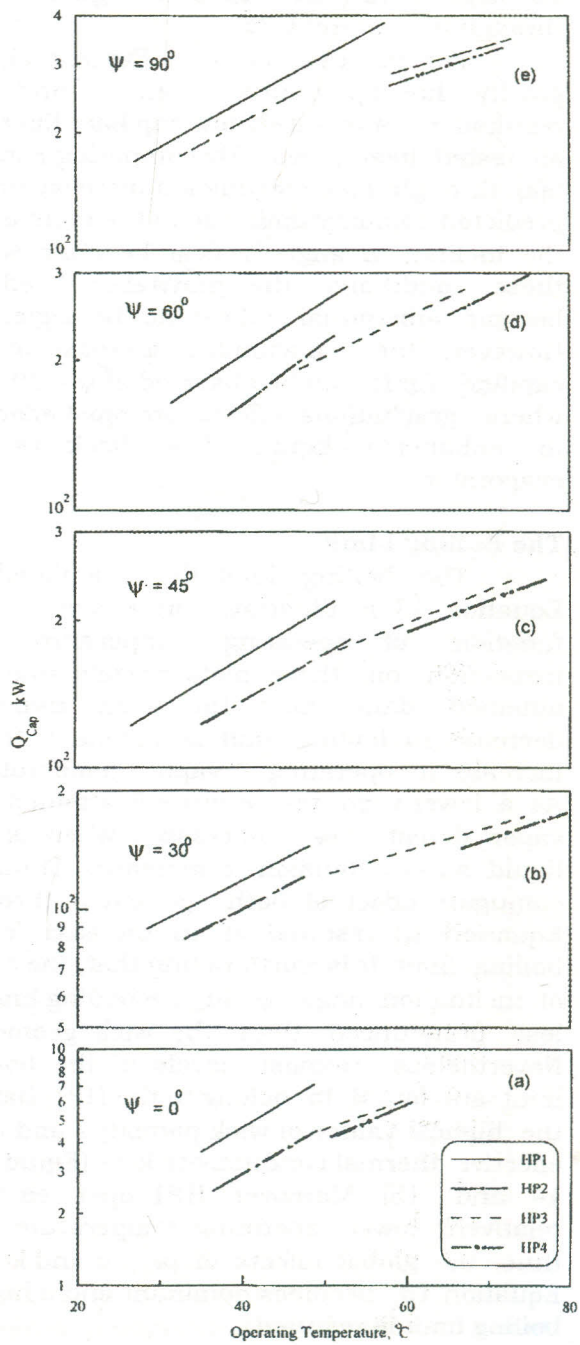

Figure 6 The capillary limit as a function of the operating temperature and the inclination angle as a parameter.

for other tested heat pipes - generates low a capillary pressure, as well as higher flow resistance in the wick. This is due to the fact that a decreased wick permeability tend, to deteriorate the wick ability to pump liquid up to the heated section. Thus a degradation of the capillary limit for these heat pipes is resulted. Results for the same tested heat pipes at inclination angles of 30, 45, 60 and 90 degrees are illustrated in Figures 6 (b) through (e), respectively.

For the case of ψ=0, Figure 6(a), the gravity has apparently no effect and this resulted in a relatively low capillary limit, for all tested heat pipes. By comparing Figures 6(a) through 6(e) a significant increase in the predicted capillary limit due to the increase in the inclination angle ψ can be observed. In these conditions, the gravitational effects become substantial and can not be neglected. However, the maximum increase of the capillary limit can be observed at ψ = 90 deg. where gravitational effects are most effective in enhancing liquid flow back to the evaporator.

The Boiling Limit

The boiling limit Q_b calculated by Equation 13 is illustrated in Figure 7 as a function of operating temperature. An inspection on these plots reveals that, all obtained data have the same trend, a decrease in boiling limit is amenable to the increase in operating - vapor - temperature. As a lower vapor temperature is attained, the vapor density ρ_v decreases whereas the liquid surface tension σ increases. Thus the conjugate effect of both ρ_v and σ through Equation 13 resulted in an increase in the boiling limit. It is worth noting that, the effect of inclination angle ψ on the boiling limit is less pronounced than the wick geometry. Nevertheless, upmost levels of the boiling limit are found to belong to the HP1, having the highest values of wick porosity ε and wick effective thermal conductivity k_{eff} - (Equations 14 and 15). Moreover, HP1 operates with relatively lower operating temperature and thus, the global effects of ρ_v , σ and k_{eff} in Equation 13, becomes dominant and a higher boiling limit is resulted.

Two performance limits Q_{cap} and Q_b are presented in Figure 8 as a function of the vapor temperature for the two tested heat pipes HP1 and HP4 for the worst conditions of ψ = 0 degree. As an exception to greater inclination angles, the boiling limit Q_b was found to be larger than the capillary limit Q_{cap}, which implies that the maximum performance of the heat pipe should be limited by the capillary limit.

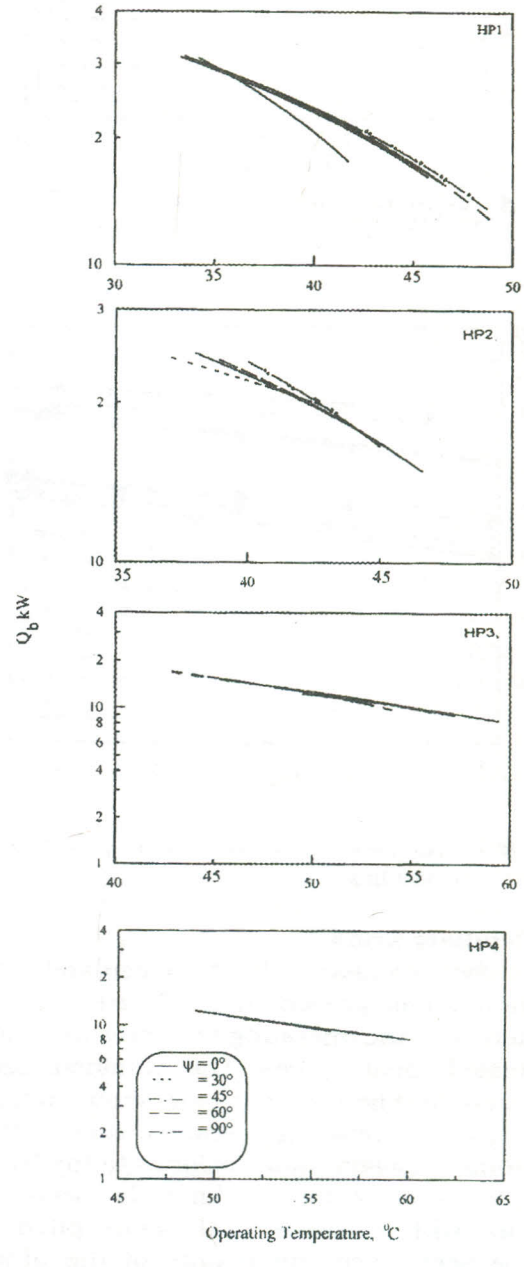

Figure 7 The boiling limit vs. the operating temperature with the inclinatiation angle as a parameter.

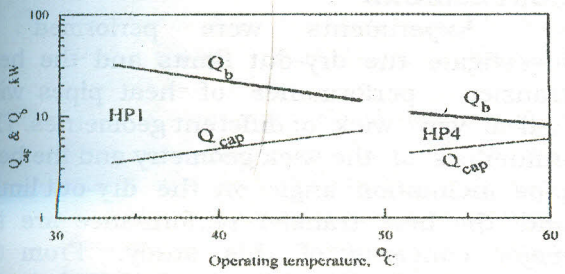

Figure 8 The capillary and boiling limits of HP1 and Hp4 at the horizontal position.

Heat Transfer Performance

It is postulated that, for a heat pipe operating below its heat transport limits, previously discussed, the performance can be characterized by the overall coefficient of heat transfer U_{HP} defined by the equation:

$$Q = A_{HP}\ U_{HP}\ (T_e - T_c) \qquad (16)$$

In Equation 16, A_{HP} is chosen as the fundamental area to obtain the value of U_{HP}. In this study, A_{HP} was taken as the heat pipe cross-sectional area.

The variation of the overall heat transfer coefficient U_{HP} with heat flux q is shown in Figure 9 for the four tested heat pipes at various inclination angles. This figure shows that; the heat transfer coefficient increases with increase in heat flux. Larger values of U_{HP} are noticed for the heat pipes operating at values of ψ larger than zero, and smaller helix pitch.

This outcome is apparently due to the gravitational effects that leads to enhance the liquid flow back to the evaporator and preventing or at least receding film evaporation.

Comparing the values of U_P for the four pipes presented in Figure 10, one can observe that the magnitude of U_{HP1} is much larger than that of the other heat pipes (having wicks of greater helix pitch). This can be explained by understanding the mechanism of bubble formation, growth and separation, which is dominated by the wick geometry. The formation of bubble occurs at the nucleation sites of the heated surface and at those locations which may be formed due to the contact of the heated surface with the wick wire. Thus, one may expect that the number of the nucleation sites is substantially increased for the HP1 having

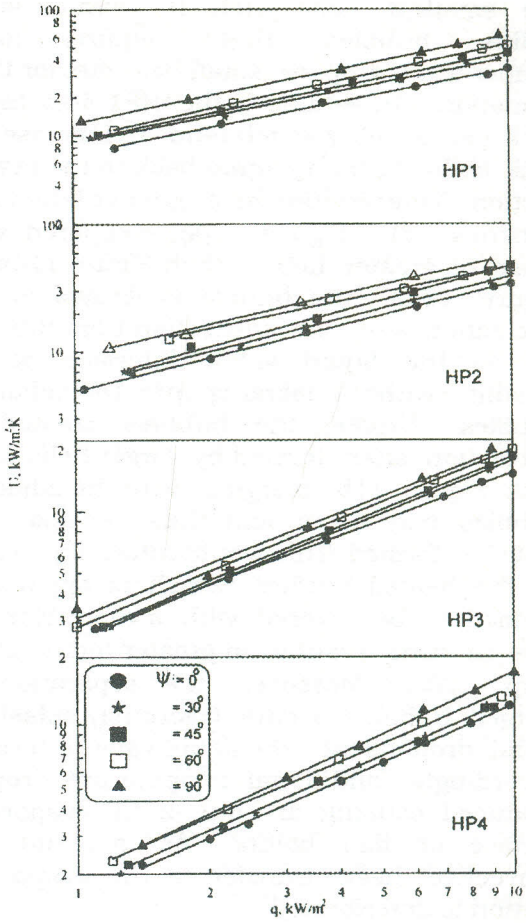

Figure 9 The overall heat transfer coefficient vs. heat flux for tested heat pipes at various orientations.

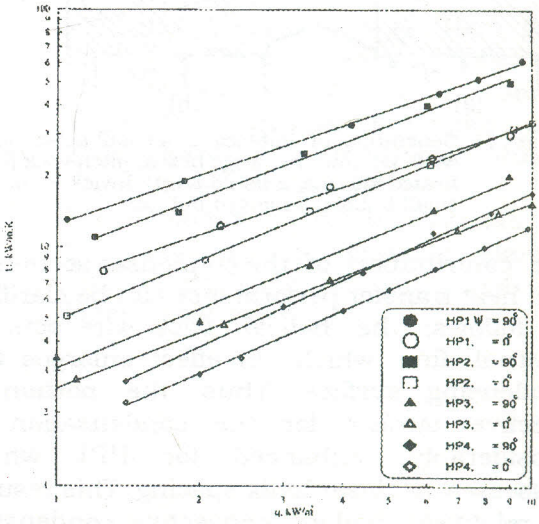

Figure 10 Comparison of heat transfer coefficients of teased pipes

the smallest helix pitch. It creates small radius bubbles that require, lower temperature drop or small heat flux for their formation .In addition, the HP1 has larger wick permeability which tends to increase the wick ability to pump liquid back to the heated section. This results in a greater liquid film thickness δ_1, Figure 11(a), compared with those of greater helix pitch Figure 11(b). In Figure 11(a), the bubble is formed at the nucleation site, the separation from this site up to the liquid vapor interface occurs steadily without merging into the adjacent bubbles. Unlike, the bubbles created at nucleation sites formed by larger helix pitch wick Figure 11b, merging with the adjacent bubbles may occur and thus, a vapor film may be formed. This would retard liquid flow to the heated surface, which is apparently seemed to be covered with a vapor blanket. This in turn, results in greater temperature drop, ΔT_{e-v}. Moreover, the separation of merged bubbles occurs vigorously splashing liquid droplets at the liquid vapor interface. Accordingly, additional temperature drop is produced causing dry out of the evaporator surface or film boiling. As a result, the convective heat transfer in the evaporator section is deteriorated.

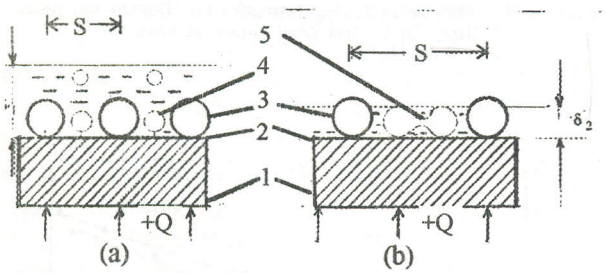

Figure 11 Generation of bubbles in a small helical pitch wick (a) and in large helical pitch wick (b) 1-heated surface, 2-liquid layer, 3-wick, 4-formed small bubble, 5-merged bubbles

The contribution of the condenser section to the heat transfer performance can be clarified as follows: the helical wick wire acts as internal fins which in effect enlarges the condensing surface. Thus, the portion of effective surface for the condensation is considerably enhanced for HP1 which possesses a closer helix spacing. This results is relatively higher convective condensing heat transfer compared with the other heat pipes of wider helix pitch.

CONCLUSIONS

Experiments were performed to investigate the dry-out limits and the heat transfer performance of heat pipes with helical wire wick of different geometries. The influences of the wick geometry and the heat pipe inclination angle on the dry-out limits and the heat transfer performance are the major concerns of this study. From the present results, the following conclusions can be drawn:

. The capillary limit is dependent on the wick geometry and the heat pipe inclination angle. It increases with the decrease in both the helix pitch , and vapor temperature. Both result in higher maximum capillary pressure. At the same time, an increase in inclination angle, leads to a larger capillary limit. This is brought about by the increasing gravitational effects tend to enhance the liquid flow back to the evaporator.

2. The boiling limit was found to increase with the decrease in both operating temperature and helix pitch. The heat pipe HP1, having smallest helix pitch, larger wick effective thermal conductivity and working at the lowest operating temperature, exhibits the highest value of boiling limit. Also, it was found that the effect of inclination angle on the boiling limit is less pronounced as opposed to the effect on the capillary limit.
3. With zero inclination angle, the tested heat pipes exhibit capillary limits lower than the boiling limits. This postulates that, the design of such devices should be characterized by the capillary limit.
4. The overall heat transfer coefficient was found to be influenced by the wick geometry and inclination angle. Comparative analysis showed that, HP1 having the smallest helix pitch operating with lower vapor temperature, and smallest temperature drops Δt_{e-c} results in highest values for heat transfer coefficient. For greater inclination angles the increased liquid flow to the evaporator was found to be the reason for the further increase in heat transfer performance.

REFERENCES

[1] Mahmoud Abo El Nasr; " Gravity Asisted Heat Pipes", Ph.D Thesis,. Ain Shams University, 1985.

[2] C.T. Crowe, A. El Ahwány, Abo El Nasr, and R. Abdel Aziz; " Performance Limits of a Porous Heat Pipe"; Proceeding of Eighth International Conference for Mechanical Power Engineering, Alexandria, pp. 253-261, 1993.

[3] Tadashi Yamamoto, and Y-Tanaka; "Experimental Study of Sodium Heat Pipes. JSME International Journal Vol. 30, No. 269, pp 1776-1782, 1987.

[4] Flavio Dobran; "Suppression of the Sonic Heat Transfer Limit in High Temperature Heat Pipes"; J. of Heat Transfer, Vol. 14, pp 605-610, 1989.

[5] B.R. Babin, G, P. Peterson, and D.Wu; " Steady-State Modeling and Testing of a Micro Heat Pipe"; J. of Heat Transfer, Vol 122 pp 595-601, 1990.

[6] M.M. Chen, and A. Faghri; "An Analysis of the Vapor Flow and the Heat Conduction Through the Liquid-wick and Pipe wall in a Heat Pipe With Single or Multiple Heat Sources"; Int. J. Heat Mass Transfer, Vol. 33, No. 9 pp 1945-1955, 1990.

[7] A. Faghri, M. Buchko, and Y. Cao; " A Study of High-Temperature Heat Pipes With Multiple Heat Sources and Sinks: Part 1- Experimental Methodology and Frozen Start-up"; J. of Heat Transfer, Vol. 113, pp 1003-1009, 1991.

[8] B.R. Bahin and G.P. Peterson; "Experimental Investigation of a Flexible Bellows Heat Pipe for Cooling Discrete Heat Sources"; J. of Heat Transfer, Vol. 112, pp 603-607, 1990.

[9] M.S. El Genk and L. Huang; "An Experimental Investigation of the Transient Response of a Water Heat Pipe"; Int. J. Heat Mass Transfer, Vol. 36, No. 15, pp 3823-3830, 1993.
Heat Pipes"; Proceeding of Numerical Heat Transfer, Part B, 25 p 331, 1994.

[11] J.M Tournier and M.S. El Genk; "A Heat Pipe Transient Analysis Model"; Int. J. Heat Mass Transfer Vol. 37, No. 5 pp 753-762. 1994.

[12] B.H. Kim and J.P. Peterson; "Analysis of the Critical Weber Number at The Onset of Liquid Entrainment in Capillary Driven Heat Pipes"; Int. J. Heat Mass Transfer, Vol. 38, No. 8, pp 1427-1442, 1995.

[13] M.P. Mughal and O.A. Plumb; "An Experimental Study of Boiling on a Wicked Surface"; Int. J. Heat Mass Transfer, Vol 39, No. 4 pp 771-777, 1996.

[14] D.A. Pruzan, L.K. Klingensmith, K.E. Torrance, and C.T. Avedisian; "Design of High-Performance Sintered-Wick Heat Pipes" ; Int. J. Heat Mass Transfer, Vol. 34, No. 6, pp 1417-1427, 1991.

[15] P.C. Stephan and C.A. Busse; "Analysis of the Heat Transfer Coefficient of Grooved Heat Pipe Evaporator Walls"; Int. J. Heat Mass Transfer Vol. 35, No.2, pp 383-391, 1992.

[16] D. Khrustalev and A. Faghri; "Estimation of the Maximum Heat Flux in the Inverted Meniscus Type Evaporator of a Flat Miniature Heat Pipe"; Int. J Heat Mass Transfer, Vol. 39, No. 9, pp 1899-1909, 1996.

[17] S.W. Ch.; "Heat Pipe Theory and Practice: A Source Book"; McGraw-Hill, 1976.

[18] P. Dunn and D.A. Reay; "Heat Pipes"; A Source Book, Pergamon Press, 1972.

[19] M.N. Ivanovski, V.P. Sorokin and I.V. Yagodkin; "Physical Principles of the Heat Pipes"; A Source Book in Russian. Atom Press Moscow, 1978.

[20] I.G. Choomac, V.P. Chepornenko, and G.G. Choklin; "Refrigeration Plants"; A Source Book in Russian, Pish Prom Press, Moscow, 1981.